Journal of Engineering and Sustainable Development
https://jeasd.uomustansiriyah.edu.iq/index.php/jeasd
https://doi.org/10.31272/jeasd.27.5.5

Vol. 27, No. 05, September 2023
ISSN 2520-0917

Original Research

COOLING OF CONCENTRATED PHOTOVOLTAICS WITH PHASE CHANGE MATERIAL AND FINS

Mostafa K. Yousif*, Muna S. Kassim

Mechanical Engineering Department, Mustansiriyah University, Baghdad, Iraq
(https://orcid.org/0009-0003-6559-3134 ; https://orcid.org/0000-0001-5742-9965)

Received 25/08/2022 ***Accepted in revised form 14/12/2022*** ***Published 01/09/2023***

Abstract: The increase in cell temperature with increased irradiance is probably the most significant disadvantage of using photovoltaic with reflector modules. In this study, a developed Phase Change Material system was integrated into the rear section of a concentrating Photovoltaic system to limit its temperature rise. The heat transmission of the concentrating photovoltaic with a phase change material system was investigated using an experimental method and a numerical method. The temperature distribution was simulated numerically using ANSYS 2021 three-dimensions model. Three cases were studied: one without wax, one with wax, and one with wax and fins. The results displayed convergence between the experimental results and the numerical results**.** The effect of using phase change materials on performance and efficiency of concentrated photovoltaic cells, the amount of temperature reduction through the wax melting period for concentration with paraffin wax and concentration photovoltaic with fin and paraffin wax by 2.8 °C and 6 °C, respectively, as well as an enhancement in efficiency of photovoltaic at the noon time of cases by 1.807% and 3.182% related to the reference photovoltaic. The outcomes also demonstrated that using fins aids in the distribution of temperatures, resulting in regular melting of wax in comparison to wax without fins.

Keywords: *ANSYS; phase change material; concentration photovoltaic; Paraffin wax; passive cooling*

1. Introduction

In commercial photovoltaics (PV), only about 5% to 25% of the solar energy incident on the solar panel can be converted into electricity and the remaining energy is converted into heat [1]. The useful life of the photovoltaic module can be reduced, resulting in long-term damage and increased temperature of photovoltaic modules [2]. The reduction in electrical efficiency results in an increase in operating temperature is determined by the material composition of the photovoltaic cell [3]. The efficiency of PV decreases around 0.5 % when the temperature of PV increases by one Kelvin for crystalline silicon-based PV systems[4], [5]. The temperature of photovoltaic energy must be regulated to improve its performance of the Photovoltaic[6]. Solar panels can be cooled in a variety of ways, including passive and active approaches [7]. Hydraulic cooling, spray cooling, and other active approaches [8]. This study discusses Using (PCM) by way of a passive cooling technique. Because of global weather changes besides water shortages [9].The phase change material is becoming gradually important. PCMs, also referred to as latent heat energy, are substances that, with only a minor temperature change, can accumulate and release a significant amount of heat during the melting process. [10]. Numerous investigations on photovoltaic modules with phase change material (PV/PCM) have been conducted. Atkin and Farid

**Corresponding Author*: *mkykt87@gmail.com*

[11] conducted an indoor experiment and numerical simulation using MATLAB program on cases (PV panel only, PV panel with PCM, PV panel with heat sink, PV panel with PCM and heat sink) to demonstrate the effect of utilizing graphite with exterior fins on photovoltaic performance, with the results revealing that case four achieved the greatest total efficiency increase (12.9%). Stropnik and Stritih [12] performed experimental studies and numerical studies to show if the paraffin wax (RT28) might be used to decrease the Photovoltaic temperature during the time. The outcomes displayed that the output power of (PV with PCM) improved by (4.30%) - (8.70%), while the electrical efficiency of the photovoltaic panel improved by (0.50%) to (1.1%). It has also increased energy production and efficiency by 7.3% and 0.8%, respectively. Tan et al. [13] implemented a numerical method to investigate the thermal performance as well as the electrical performance of a photovoltaic that was chilled using paraffin wax has a melting point of 27 °C and fins. The investigators were concerned about the effectiveness with which the PV system cooled the system. In comparison with naturally air-cooled photovoltaic systems,, the results presented that a PV+PCM with a twelve-fin arrangement can decrease Photovoltaic cells temperature by about 15 °C while increasing efficiency by 5.39 °C. Sharma et al. [14] improved the overall performance of a low-concentration system by using phase change material (LCPV). When these materials were added to a CPV system with natural ventilation and no PCM, the average temperature of the solar units was reduced by 3.8 ° C. Wei Lu et al. [15] directed numerical studies and (indoor) experimental studies, and the results displayed that the temperature of concentration photovoltaic with wax (PCM) systems with parallel aluminum fins is around (3)° C lesser than the temperature of a PV panel with PCM without fins. While the phase change material melts, this temperature can be sustained for extra than five hours. Su et al. [16] investigated a tracking use with (CPV-T) system that utilized water for system cooling and immersed encapsulated PCM spheres as the concentrating medium. According to the findings, the average gains in thermal efficiency, electrical efficiency, and total efficiency of the CPV-T system using phase change material are 5%, 10%, and 15% higher, respectively .Emam and Ahmed [17] looked at how four different type of phase change material with heat sink configurations affected the thermal manager of a CPV system. The study found that the temperature of a solar cell drops significantly when there are more fins on it. Optimizing phase change material patterning is an important aspect of managing temperature in Concentration PV-PCM systems. Savvakis et al. [18] used a tubular shape in an experimental study in Mediterranean settings. When 260 grams of PCM (RT27) and (RT31) use, the Maximum temperature decreases were (6.4 and 7.5) ° C, while improvements in power were 4.19% and 4.24%, respectively. Despite a 2% increase in PV/PCM efficiency. Wongwuttanasatian et al. [19] investigated tests to determine whether palm wax could control the temperature of an air-based photovoltaic collector using finned, tubed, and grooved PCM containers, compared to the other containers, the finned container cooled more effectively, reducing the photovoltaic temperature by 6.1 ° C and improving its electrical efficiency by 5.3%. Shasatry and Arunchala [20] conducted an experimental study to try to improve PV/T performance by using an aluminum matrix in a PCM container to improve heat transfer and accelerate the amount at which it liquefied and solidified. The efficiency of photovoltaic panels with an aluminum matrix and PCM increased by 8.6% and 3.5%, while the temperature was

reduced by 11.1% and 7.9%, respectively. Rajan Kumar et al. [21] Three different types of photovoltaics were put through experimental investigations in hot weather to see how well they performed: the photovoltaic reference (module 1), the photovoltaic using PCM (module 2), and the photovoltaic with PCM packed in a container with exterior fins (module 3). The electrical performance improved by 5.16% and 6.59% while PV temperature decreased by 12 ℃ and 22.3°C, respectively, in modules (2 and 3). Qasim et al. [22] carried out experimental research to improve the performance of a photovoltaic panel system. Two types of PCM were employed, with varying numbers of fins. The outcome shows that the use of fins with numbers (two, five, eight, and eleven) reduces the temperature of the photovoltaic panel by (23.80, 24.20, 25.10, and 26.60) ° C and increases electrical efficiency to 11.2%, 11.7%, 11.9%, and 12.1%, respectively. Furthermore, utilizing one type of PCM is better than two types. Reduced the temperature around (9.60 and 7.80) °C, respectively. In comparison to normal Photovoltaic. Sharma et al. [23] implemented an experimental study to enhance the performance and efficiency of a concentration photovoltaic system (CPV) using passive way cooling with various phase change materials (RT28HC and RT50). The results displayed an increase in electrical energy production by 17% at PCM type (RT28HC) and 19% at PCM type (RT50) when compared to natural ventilation. Ahmadi et al. [24] examined the performance of the passive method in addition to the air cooled by the embedded carbon foam in the PCM materials and the water passing below the photovoltaic system under a variety of solar irradiation situations. The PCM composite improved PV electrical efficiency by 14% by using passive cooling to reduce PV temperature by 6%, the thermal efficiency of this active cooling system is 81.6%. Vaziri Rad et al [25] investigated the thermal performance of water-based PV/T using (salt hydrate) and aluminum shavings as a porous media. When compared to the reference photovoltaic, the proposed approach reduced temperature by 24 °C while improving electrical performance by 2.5%. Aluminum shavings accelerated PCM melting by 25%. Over the reference PV, the proposed system increased exergy efficiency by 4.43%. Siddharth S. Patil, et al [26] conducted an experimental investigation to control the temperature of a photovoltaic panel. According to the study, the use of PCM and fins was successful in keeping the temperature of the photovoltaic panel below 50 °C. Fins and PCM reduced average PV panel temperature by 7-10 degrees Celsius, increasing efficiency from 1.4% to 4.6%.

In this study, concentrated photovoltaic cells, a type of concentrator with low concentration and phase change materials for passive cooling, were used. The primary objective of this paper is to illustrate the result of using PCM on the performance of photovoltaic cells.

2. Experimental Approaches

2.1 Phase Change Material Selected

There were several different materials investigated for use as phase change materials. Overall, salt hydrate has a shorter lifetime cycle and exhibits a supercooling phenomenon when related to other materials. On the other hand, micro-condensed phase change materials are easily combined but require constant moving. The results of previous investigations showed these characteristics of salt hydrate. Paraffin wax is a chemically constant PCM that has the potential to produce a relatively constant thermal performance throughout a long-term operation [27]. In addition, the typical working temperature of PV is 25 °C, and it has been shown that

operating PV cells at temperatures greater than this might have a negative impact on their efficiency [2]. Taking these parameters into account, Iraqi paraffin wax was decided as the most suitable phase-transition material for the present investigation. The transition temperature for this PCM is 56 °C. Table 1 provides a summary of the thermophysical characteristics of paraffin that are considered.

to be the most essential.

Table 1. The specifications of PCM

properties	values
Melting point	56
Heat of fusion	226
Specific heat	2.95/2.51
Density solid/liquid	818/760
Thermal conductivity	0.24/0.24

The PCM (paraffin wax) container revealed in Fig. 1 is a rectangular box with 9 fins attached to the front aluminum plate. The fins are (7) cm apart from each other. The PCM container with dimensions (62.5cm, 42.5cm, 3cm). Silicon was used to seal the container to prevent wax leakage from the PCM container. A 2-mm-thick aluminum plate was attached to the front of the PCM container. This makes it easier for heat to move between the photovoltaic panel and the PCM (paraffin) container. A 2 mm thick aluminum plate was used to cover the back of the container. To keep the melted PCM from leaking out of the container, a silicone sealant and a screw were put between the walls of the container and the aluminum plates.

(A)

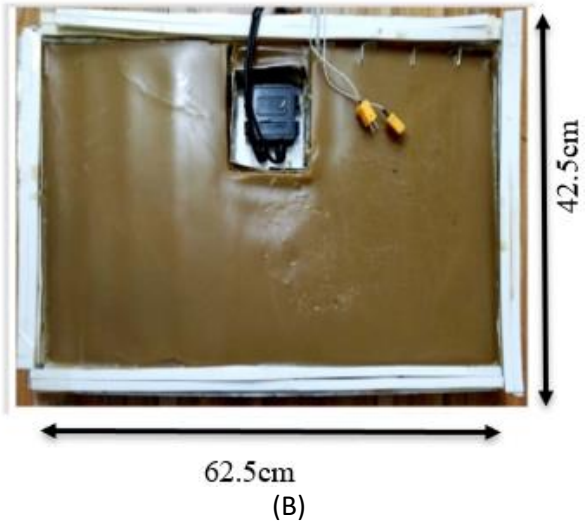

(B)

Figure 1. A: Container without PCM.
B: Container with PCM.

2.2 Experimental Setup

The experiment was carried out outdoors to study the impact of PCM on the cooling of the CPV. The experiment was carried out with two concentrated photovoltaic panels one without PCM (CPVI) and the other with PCM and fins (CPV/FPCM), as illustrated in Fig. 2. The photovoltaic is installed at a 30° angle to the horizon, with aluminum foil reflectors the same size as the photovoltaic cell installed at a 120° angle to the cell surface. EURONET Monocrystalline solar panel 40-watt photovoltaic cells with dimensions (670 * 425*25) mm

Figure 2. Experimental photovoltaic concentration rig with PCM and fins.

The experiment was carried out in Baghdad City from 8 a.m. to 5 p.m. in May 2022. The solar radiation intensity meter measured the amount of solar radiation that dropped on the PV panel. A K-type thermocouple was used to measure the photovoltaic and ambient air temperatures installed on the surface of the solar panels. Temperatures were manually recorded every hour for the period from (8 a.m.) to (5 p.m).

2.3 Uncertainty Analysis

Uncertainty analysis is required to assure the accuracy of exam results and to avoid measurement mistakes. Table 2 shows the accuracies of several measuring devices. The uncertainty parameter is computed using the equation below, as reported by Kline et al. [27]:

$$\omega x = \sqrt{\left(\frac{\partial R}{\partial X_1}\omega_{X_1}\right)^2 + \left(\frac{\partial R}{\partial X_2}\omega_{X_2}\right)^2 + \cdots + \left(\frac{\partial R}{\partial X_n}\omega_{X_n}\right)^2} \quad (1)$$

Table 2. Accuracy of Measuring Devices

item	Thermocouple at the PV surface(°C)	PV voltage	PV current
Average standard uncertainty	$\mp$ 0.5	$\mp$ 0.4	$\mp$ 0.25

In equation (1), R is the function of independent variables (x_1, x_2, …x_n) and ω_R is the uncertainty of R. Also, ω_{x1}, $\omega_{x2,}$ and ω_{xn} indicate the uncertainty of the independent variables.

3. Numerical Analysis for CPV/PCM

Three models were investigated to show the impact of adding fins: the concentration photovoltaic model without PCM, the concentration photovoltaic model with PCM (CPV/PCM), and the concentration photovoltaic model with PCM and fins (CPV/FPCM), as shown in Fig. 3.

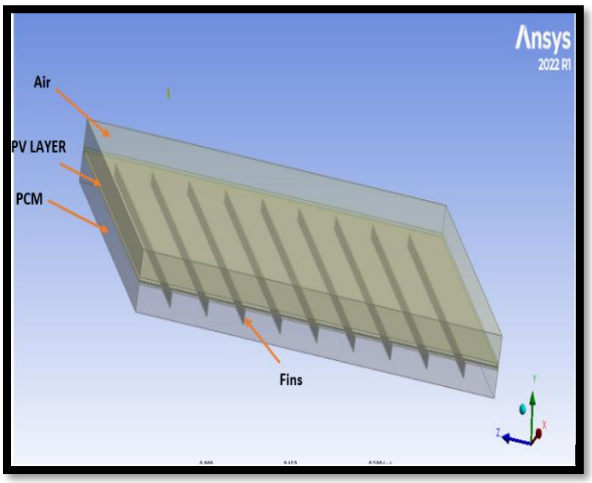

Figure 3. Geometry of the CPV/FPCM model.

The geometry of each model is built using ANSYS Design Modeler. A glass, a silicon layer, an EVA layer up, an EVA layer down, and a Tedlar layer PCM are enclosed in an aluminum container that is close to the Tedlar layer of PV. The parameters of the PV layers and container properties are revealed in Table (3).

Table 3. Properties of photovoltaic

Component	ρ $(Kg.m^{-3}$	Thickness mm	C_p $(j.kg^{-1}k$
silicon	2330	0.3	680
EVA	960	0.5	2100
glass	3000	3	500
AL	2719	2	871
Tedlar	1200	0.1	1250

3.1 Governing Equations of the PV/FPCM System

3.1.1 Solid components

Conduction is the only mode of heat transfer that is possible in solid parts such as glass layer, silicon, EVA up, EVA down, Tedlar, and PCM containers. Because of the narrow operating temperature range, photovoltaic layers are thought to have thermal properties that are isotropic and do not depend on temperature in any way. The following is the energy equation that applies to all components:

- The energy equation:[28]

$$\frac{\partial}{\partial t}(\rho H) + \nabla.\left(\rho \vec{V} H\right) = \nabla.(K\nabla T) \quad (2)$$

3.1.2 Phase change material (PCM)

During the thermally activated process, the solid phase of the PCM slowly changes into the liquid phase of the PCM. Here are the controlling equations [29] for 3 D CPV/PCM system model:

- The continuity equation:

$$\frac{\partial \rho}{\partial t} + \nabla.\left(\rho \vec{V}\right) = 0 \quad (3)$$

- The momentum equation:

$$\rho \frac{\partial \vec{V}}{\partial} + \rho\left(\vec{V}.\nabla\right)\vec{V} = -\nabla p + \mu\nabla\vec{V} + \rho\beta\vec{g}(T - Tref) + \vec{S} = 0 \quad (4)$$

The material's enthalpy is equal to the summation of sensible enthalpy (h) and latent heat (ΔH);

$$H = h + \Delta H \quad (5)$$

$$h = h_{ref} + \int_{T_{ref}}^{T} C_P dT \quad (6)$$

The amount of liquid fraction for PCM (α) can be found as shown below:

$\alpha = 0$ if $T < T_S$

$\alpha = 1$ if $T > T_I$

$$\alpha = \frac{T - T_S}{T - T_I} \quad If\ T_S < T < T_1 \quad (7)$$

The latent heat (h) can then be set as L, which stands for the material's latent heat (ΔH);.

$$\Delta H = \alpha L \quad (8)$$

The enthalpy porosity method looks at the mixture area (the area that has only partially hardened). Porosity is set.

$$\vec{S} = \frac{(1-\alpha)^2}{(\alpha^3+\varepsilon)} A_{mush}\, \vec{V} \quad (9)$$

Where ε is represented on a (0.001) to avoid zero, A_{mush} is the wax zone.

3.2 Boundary Conditions

All of the solid components of system CPV/PCM, including the various layers of PV, Paraffin, as well as aluminum, are assumed to have a primary temperature of 37°C. It is considered that heat is transferred to the surrounding air by convection and radiation from the front and rear surfaces., respectively, as shown in Fig.4.

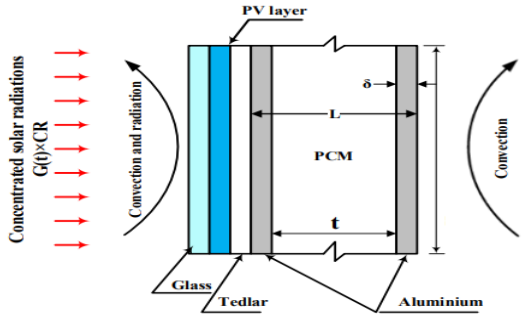

Figure 4. Schematic diagram with boundary condition.

3.3 Assumptions

In order to carry out the numerical simulation, the following assumptions were used:

1. It was presumed that the heat flux was spread evenly throughout the PV cells.

2. It was hypothesized that the PCM was both isotropic and homogeneous.
3. The effect of changes in PCM density Boussinesq approximation.
4. The movement of the liquid stage transition material was incompressible, laminar, and unsteady at the same time.
5. The expansion of space that occurs during the transition from the solid phase to the liquid phase was not taken into account. The Boussinesq approximation, which is a common assumption to include buoyancy for natural convection, was utilized even though the model does not take into account the space expansion that occurs consequently of a change in density.

3.4 Numerical Model

In general, any model that incorporates CFD (fluent) will go through several rounds of analysis. This model's representation goes over four steps: geometry drawing, meshing, setup processing, and outcomes analysis. The model was built together using the commercial programmer ANSYS.

Four photovoltaic layers and PCM zones with the same inside dimensions as the experimental test section were produced in an accurate 3D model in ANSYS. The solidification and melting model are activated for PCM's melting and solid processes, and the mushy zone constant in software is put at 10^6, which performs well in most situations. This model is operated using the enthalpy porosity method. FLUENT automatically turns on the energy equation when this model is activated.

The initial step after exporting a mesh file is to inspect the mesh for errors. The next step is to select a transient solution on a pressure basis. In fin PCM, the pressure velocity coupling equations were derived using the (SIMPLE) method for solving pressure-related equations. The momentum and energy equations were solved using power law, and the pressure correction, velocity, thermal energy, and liquid fraction were evaluated using the first-order upwind technique. The convergence criteria to the continuity energy, momentum, and discrete ordinary (DO) radiation equations are default.

The governing equations were solved using ANSYS-fluent. A transient solver was utilized to solve the numerical equations. The PERESTO pressure technique was implemented. The first-order upwind technique is believed to be capable of estimating the energy, momentum, and discrete ordinate equations. The simulations were carried out with a time step of 0.5 s.

3.5 Grid Independence Study

The independent mesh study is needed because there is a relation between the speed and accuracy of numerical analysis. In this study, a hexahedron element was used for making mesh, in a grid independence test, the meshes with (516,168) (1,075,508), and (3,123,219), cells were compared. The results of the mesh with (1,075,508) cells and the mesh with (3,123,219) cells were the same as shown in Fig. 5 and appendix (A-1). Thus, a lower mesh density was selected to shorten the calculation time.

It has been discovered that choosing the number of elements to be with a time step of 0.5 seconds is an appropriate choice and that raising the element number does not have a noticeable effect on the results.

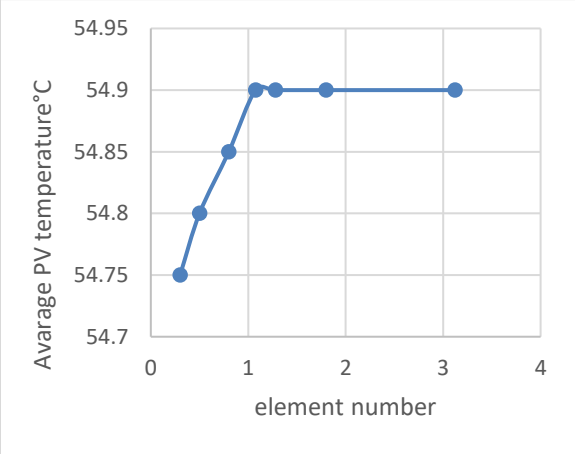

Figure 5. Mesh independence study results.

4. Model Validation

In this section, we present an analysis of the changes between the experimental data and numerical results. The experiment's settings were matched in a similar condition to maintain accuracy. The following figures show the results obtained by experimental and numerical analysis.

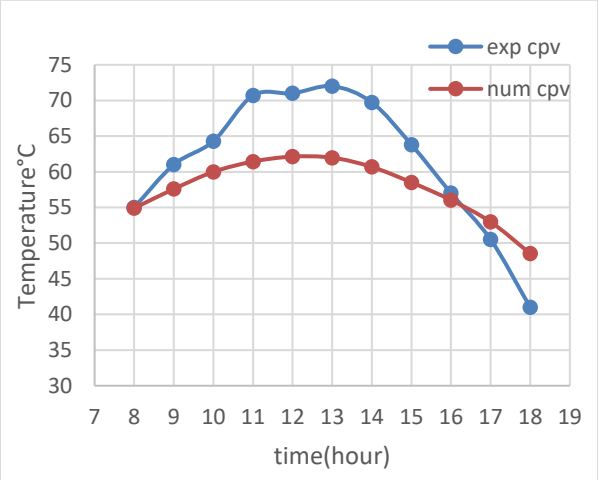

Figure 6. Comparison between the numerical results and the experimental results of conventional CPV.

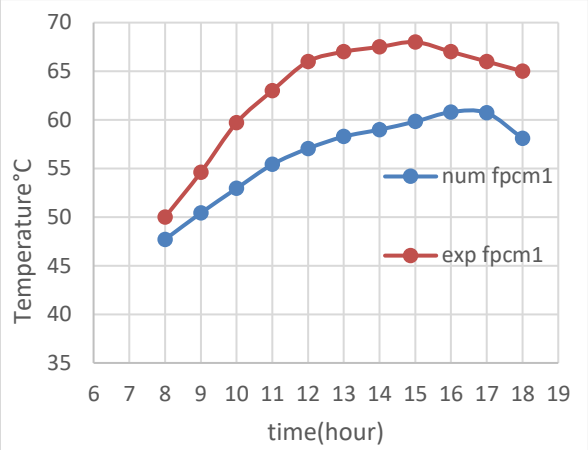

Figure 7. Comparison between experimental results and numerical results of conventional CPV with PCM and fins.

Fig.6 and Fig.7 show a comparison of the experimental and numerical results for CPVI. The numerical results agree well with the experimental data. There is a satisfying convergence between the numerical solution (CFD) and the experimental work. The highest difference between numerical and experimental results is 15.09% and 15.5% for photovoltaic cell surface temperature.

5. Results and Discussions

5.1 The Impact of Using Fins on Photovoltaic Temperature

In this sector, the effect of the addition of fins to the wax (PCM) container is studied. It causes an increase in the contact area with the wax, and the heat is transferred to the PCM parts regularly. This causes the temperature of the front PV surface to fall and remain constant range for longer time.

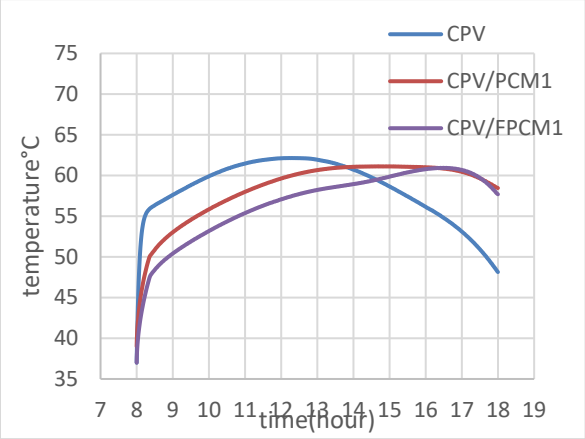

Figure 8. Average surface temperatures of CPV, CPV/PCM, and CPV/FPCM.

Fig. 8 shows the average surface temperatures of CPV, CPV/PCM, and CPV/FPCM. In general, in the morning the surface temperature is almost the same in all cases because the wax is still in the solid state and has not begun to melt yet, it can be seen that the surface temperatures of the different cases are different, Once the wax has melted. It was discovered that the CPV index temperature was greater than in the other cases. This occurs as a result of heat transmission from the back CPV to the paraffin, which causes the PCM to gradually warm up, especially in the layers that come into contact with the CPV surface. This growth spreads to the other PCM layers as the melting process progresses. Due to paraffin's capacity to hold onto heat for a while, when the PCM has completely melted, the temperature of the PV with casings containing PCM rises in comparison to the solar panel.

According to Fig. 8, it is clear that the amount of decrease in the temperature after using paraffin wax (CPV/PCM) is fewer than the CPV without wax by 2.8 ° C for the time from (8.30 am to 1 pm) and the temperature of PV in time (2 pm) is (61°C) Following that, the temperature of the panel rises due to the complete melting of the paraffin wax. The figure shows that when fins (CPV/FPCM) are used, the rate of temperature reduction (6°C) relative to the CPV reference is equal in time (2.30 PM) to temperature (59°C), after which the temperature of the CPV/FPCM rises higher than the CPV and then begins to fall due to wax retention temperature for a specific period.

5.2 Melting of Phase-Change Material process

Fig.9 illustrates the mechanism of the melting process of paraffin wax. This graphic shows that the melting process occurs after (43 minutes), where in both situations the melting percentage is the same at first, but over time. the effect of including fins, where the amount of melting rises in the event of utilizing fins compared to wax without fins. When the fins are used at the time (4 PM), they completely melt.

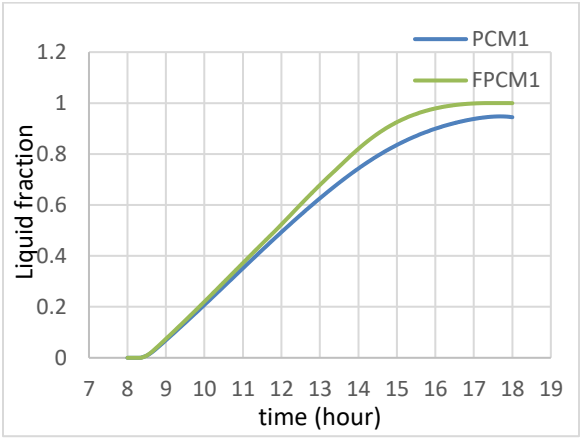

Figure 9. Liquid fraction of PV/PCM & PV/FPCM.

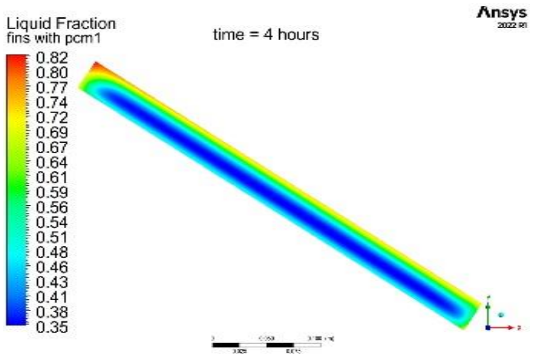

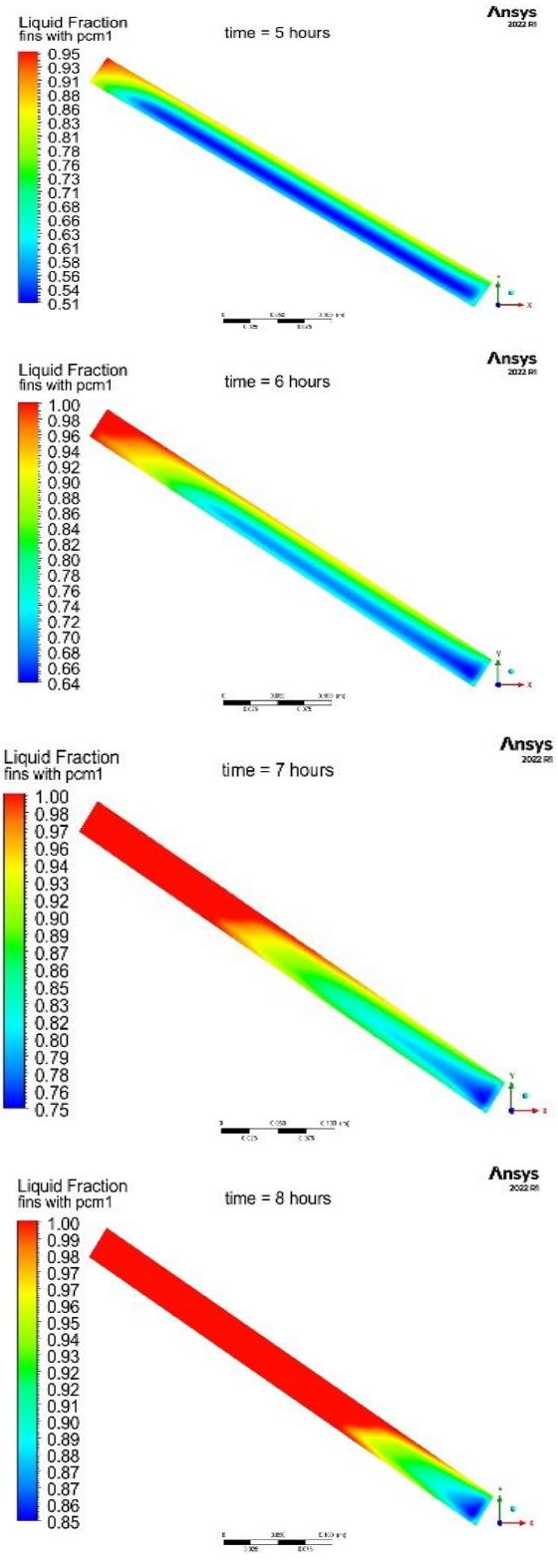

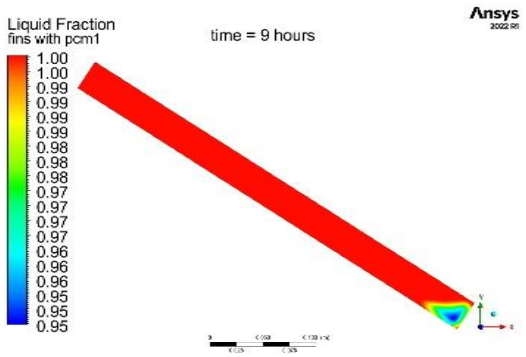

Figure 10. Liquid fraction for PCM with fins with time in MAY.

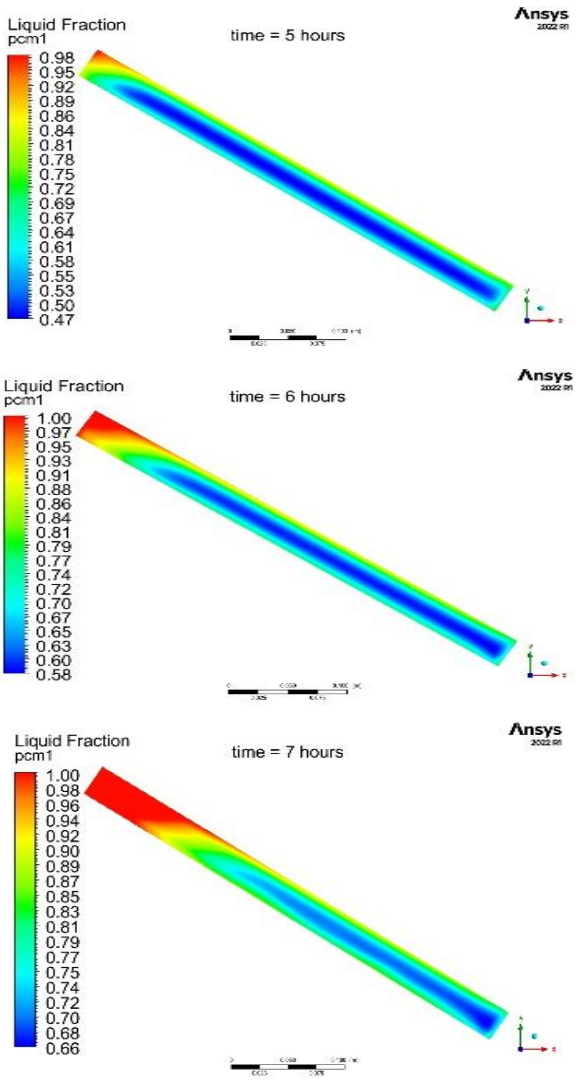

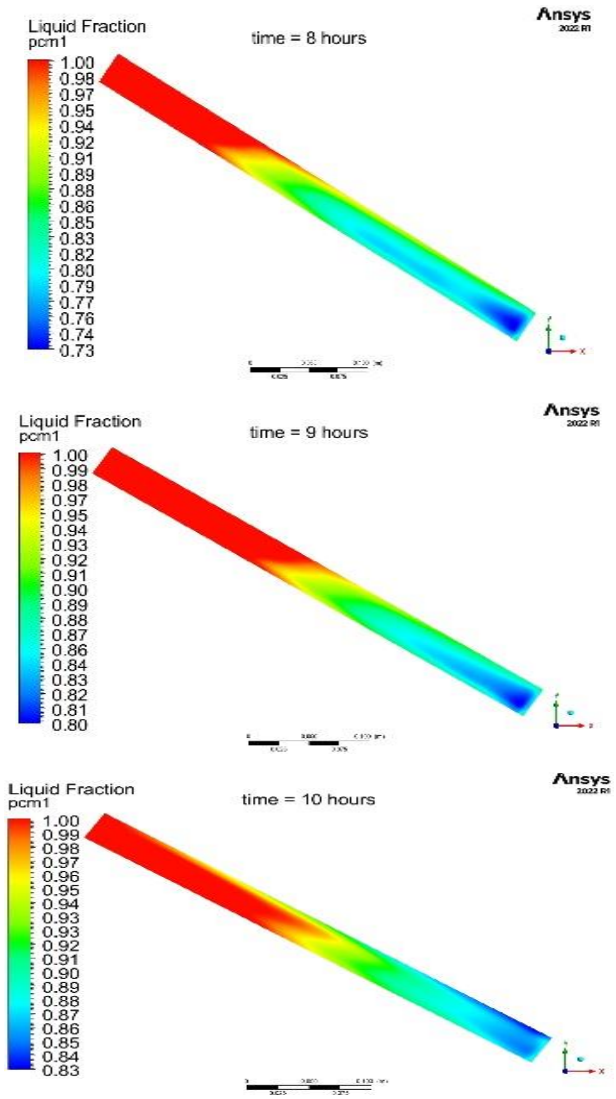

Figure 11. Liquid fraction in photovoltaics with PCM with time in May.

Fig. 10 and Fig.11 show the liquid fraction counters for the two cases (CPV/FPCM) (CPV/PCM) during the analysis period. These contours above were taken in the XY plane in the midpoint of the solar panel. The contours show the gradual melting of the wax. The melting is in a faster state, as the melting is incomplete in the case CPV/PCM. In the case of CPV/FPCM, the paraffin is completely melted during analysis.

6. Efficiency of CPV

The efficiency of system CPV depends on the temperature of the solar panel, which is considered using equation (10) below:

$$\eta_{sc} = \eta_{ref}(1 - \beta_{ref}(T_{sc} - T_{ref})) \quad (10)$$

Fig. 12 shows the efficiency of the cases (CPVI, CPV / PCM, CPV / FPCM) over time. These cases have a high efficiency before noon due to lower temperatures, which gradually fall as CPV temperatures rise. and that the development in efficiency at (12 p.m.) of cases (CPV/PCM, CPV/FPCM) is (1.807% and 3.182%), respectively, compared to the efficiency of PVI.

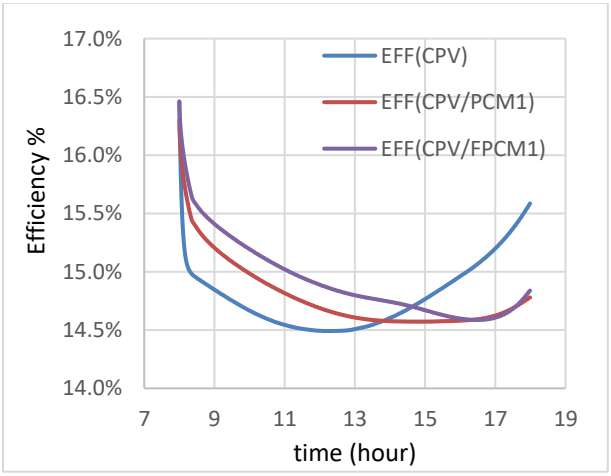

Figure 12. Efficiency of (CPVI, CPV/PCM, CPV/FPCM).

7. Conclusions

In this research paper, the thermal performance of concentration photovoltaic with the PCM system (CPV/PCM) was studied experimentally (outdoors) and numerically using ANSYS. Experimental work was performed using two systems: a concentration photovoltaic cell system without any addition (CPV) and a concentration photovoltaic cell with PCM and fins (CPV / FPCM). The simulation was carried out (3D) using ANSYS program for cases, CPV without any addition, CPV with the addition of wax (CPV/PCM), and CPV with wax and fins (CPV/FPCM). The experimental results and the numerical results were compared. The effect of using fins with wax on the melting process and heat distribution was studied during the three cases.

The use of phase-changing materials with the concentrating photovoltaic cell (CPV) can reduce temperatures during the wax melting period; the rate of temperature reduction when adding wax CPV/PCM and when adding wax and fins CPV/FPCM is (2.8°C) and (6°C), respectively. After the wax was completely melted, the temperature increased compared to the temperature of the photovoltaic cell without wax, due to the ability of wax to maintain temperatures.

The use of fins with PCM wax helps to distribute heat and melt the wax evenly throughout the wax; the improvement in efficiency at the peak time (12 PM) of the cases (CPV/PCM, CPV/FPCM) is (1.807% and 3.182), respectively, compared to the efficiency of PVI.

Author Contribution Statement

Each author put presented a research question, created a research model, and computed the findings. They contributed to the final manuscript and talked about the results.

Acknowledgements

The authors acknowledge the help and support of Mechanical Engineering Department, Mustansiriya University, and the provision measuring devices to complete this work.

Conflict of interest

According to the authors state that there are no conflicting interests involved.

Abbreviations

T	Temperature of PV
H	sensible enthalpy
h	latent heat
α	Liquid fraction
PCM	Phase change material
ρ	Density
CPV	Concentration photovoltaic
PV	Photovoltaic

References

1. S. Sharma, L. Micheli, W. Chang, A. A. Tahir, K. S. Reddy, and T. K. Mallick (2017). *Nano-enhanced phase change material for thermal management of BICPV*. Appl Energy. Vol.208, pp. 719-733 https://doi.org/10.1016/j.apenergy.2017.09.076

2. K. Kant, A. Shukla, A. Sharma and P. H. Biwole. (2016). *Thermal response of polycrystalline silicon photovoltaic panels: numerical simulation and experimental study*. Solar Energy. vol. 134, pp. 147–155, 2016, https://doi.org/doi.org/10.1016/j.solener.2016.05.00.

3. M. Chandrasekar, S. Rajkumar, and D. Valavan. (2015). *A review on the thermal regulation techniques for non-integrated flat PV modules.* Energy Build, vol. 86, pp. 692–697, https://oi.org/10.1016/j.solener.2016.05.00doi.org/10.1016/j.enbuild.2014.10.071.

4. Radziemska. (2004). novelty Bayesian method for unsupervised learning offinite mixture models', Proceedings of International Conference on Machine Learning and Cybernetics, vol. 6. pp. 3574–3578, 2004. https://doi.org/doi.org/10.1109/icmlc.2004.1380410

5. A. Kadhim Khudadad, F. Alwan Saleh, and N. Kareem Kasim, (2022). *Photovoltaic Thermal System* Direct Contact Journal of Engineering and Sustainable Development. pp. 53– no. 567Vol. 26, https://doi.org/10.1109/icmlc.2004.138041010.31272/jeasd.26.5.5.

6. S. Nieti, A.M. Papadopoulos and E. Giama, (2017). *Comprehensive Analysis and general economic-environmental evaluation of cooling techniques for photovoltaic panels, Part I: passive cooling techniques*', Energy Convers Manage, vol. 149, pp. 334–354. https://doi.org/10.1016/j.enconman.2017.

7. B. X. Jun Donga, Xiaoru Zhuanga, Xinhai Xua , Zhihuai Miaoc, (2018). *Numerical analysis of a multichannel active cooling system for densely packed concentrated photovoltaic cells* https://doi.org/10.1016/j.enconman.2018.01.081

8. F. M. Abed, M. S. Kassim and M. R. Rahi, (2017). *Performance improvement of a passive solar still in water desalination*. International Journal of Environmental Science and Technology. vol. 14, no. 6, pp. 1277–1284. https://doi.org/10.1007/s13762-016-1231-9

9. A. Venkatalaxmi (2004), *A note on the general solution of Stokes equations.* Acta Mechanica Sinica / Linxue Xuebao, vol. 32, no. 6. pp. 1044–1045. https://doi.org/10.1007/s10409-016-0601-3.

10. M. M. F. Peter Atkin, (2015) *Improving the efficiency of photovoltaic cells using PCM infused graphite and aluminium fin.* vol. 114, pp. 217–228. https://doi.org/10.1016/j.solener.2015.01.03.

11. U. S. Rok Stropnik, (2016). *Increasing the efficiency of the photovoltaic panel with the use of PCM'*, Renew Energy, vol. 97, pp. 671–679. https://doi.org/10.1016/j.renene.2016.06.011

12. S. Lippong Tana, Abhijit Datea, Gabriel Fernandesa, Baljit Singhb, (2017). Efficiency gains of the photovoltaic system using latent thermal heat energy storage', in 1st International Conference on Energy and Power, pp. 83–88. https://doi.org/10.1016/j.egypro.2017.03.110

13. T. K. M. Shivangi Sharma a, n, Asif Tahir a, K.S. Reddy b, '*Performance enhancement of a building-integrated concentrating photovoltaic system using phase change material', Solar Energy Materials & Solar Cells Journal homepage*, vol. 149, pp. 29–39, https://doi.org/10.1016/j.solmat.2015.12.035

14. M. Y. Wei Lua, Zhishan Liua, Jan-Frederik Florb, Yupeng Wub2018, *'Investigation on designed fins-enhanced phase change materials system for thermal management of a novel building integrated concentrating PV'*, vol. 225, pp. 696–709. https://doi.org/10.1016/j.apenergy.2018.05.030

15. Y. Su, Y. Zhang and L. Shu, (2018). *Experimental study of the use of phase change material cooling in a concentrated photovoltaic thermal solar tracking system', S*olar Energy, vol. 159, pp. 777-785, https://doi.org/10.1016/j.solener.2017.11.04.

16- M. A. Mohamed Emam, (2018), '*Cooling concentrator photovoltaic systems using various configurations of phase change material heat sink.* Energy Conversion

and Management journal, vol. 158, pp. 298–314 Contents. https://doi.org/10.1016/j.enconman.2017.12.077.

17. T. T. Nikolaos Savvakis, Evangelia Dialyna, (2020.) *Investigation of the operational performance and efficiency of an alternative PV + PCM concept, Nikolaos.* academia Accelerating the world's research, vol. 211, pp. 1283–1300. https://doi.org/10.1016/j.solener.2020.10.053

18. T. Wongwuttanasatian, T. Sarikarin, and A. Suksri (2020). *Performance enhancement of a photovoltaic module by passive cooling using phase change material in a finned container heat sink*. Solar Energy, vol. 195. pp. 47–53. https://doi.org/10.1016/j.solener.2019.11.05.

19. D.M.C. Shastry, and U.C. Arunachala (2020). *Thermal management of the photovoltaic module with embedded metal matrix PCM. J* Energy Storage, vol. 28, p. 101312, 2020, https://doi.org/10.1016/j.est.2020.101312

20. R. S. B. Rajan Kumar, Paidi Praveen, Samikhshak Gupta, Juttu Saikiran. (2020). *Performance evaluation of photovoltaic module integrated with phase change material filled container with external fins for extremely hot climates*. J Energy Storage, vol. 32, p. 101876. https://doi.org/10.1016/j.est.2020.101876

21. M. M. Qasim, Muhammad Arslan; Ali, Hafiz Muhammad; Khan, Muhammad Niaz; Arshad, Nauman; Khaliq, Danyal; Ali, Zarghoon; Janjua, (2020). *The effect of using hybrid phase change materials on the thermal management of photovoltaic panels – An experimental study*. ScienceDirect Solar Energy, vol. 209, pp. 415–423. https://doi.org/10.47391/jpma.256.

22. S. Sharma, N. Sellami, A. A. Tahir, T. K. Mallick and R. Bhakar. (2021). *Performance improvement of a CPV system: Experimental investigation into passive cooling with phase change materials.* Energies, vol. 14, no. 12. https://doi.org/10.3390/en14123550.

23. M. M. b a Rouhollah Ahmadi, Farhad Monadinia (2021). *Passive/active photovoltaic-thermal (PVT) system implementing infiltrated phase change material (PCM) in PS-CNT foam',* Solar Energy Materials and Solar Cell. vol. 222, p. 110942. https://doi.org/10.1016/j.solmat.2020.11094

24. A. K. Mohammad Amin Vaziri Rad, Alibakhsh Kasaeian, Soroush Mousavi, Fatemeh Rajaee, (2020). *Empirical investigation of a photovoltaic thermosystem with phase change materials and porous aluminium shavings*. Renew Energy. vol. 167, pp. 662–675. https://doi.org/10.1016/j.renene.2020.11.135

25. S. & A. B. S. siddharth S. Patil, (2021). *Performance Improvement and Cooling of the Solar Photovoltaic Panel by Using Fin and PCM Integrated Fin.* SPRINGER, pp. 151–163. https://doi.org/10.1007/978-3-030-69925-3_15

26. A. Zhongzhu; Ma, Xiaoli; Li, Peng; Zhao, Xudong; Wright, (2017). *Micro-encapsulated phase change material*

(MPCM) slurrie. Renewable and Sustainable Energy. vol. 77, pp. 246–262. https://doi.org/10.1016/j.rser.2017.04.001

27. C.K. Zelin Xu. (2014). *Concentration photovoltaic-thermal energy cogeneration system using nanofluids for cooling and heating*. Energy Convers Manag, vol. 87, pp. 504–512. https://doi.org/10.1016/j.enconman.2014.07.047

28. R. BRENT A D, VOLLER V R. (1988). *technique for modelling convection-diffusion phase change, A. to the melting of a pure metal* [J]. Numerical and 13(3): 297−318. https://doi.org/10.1080/10407788808913615

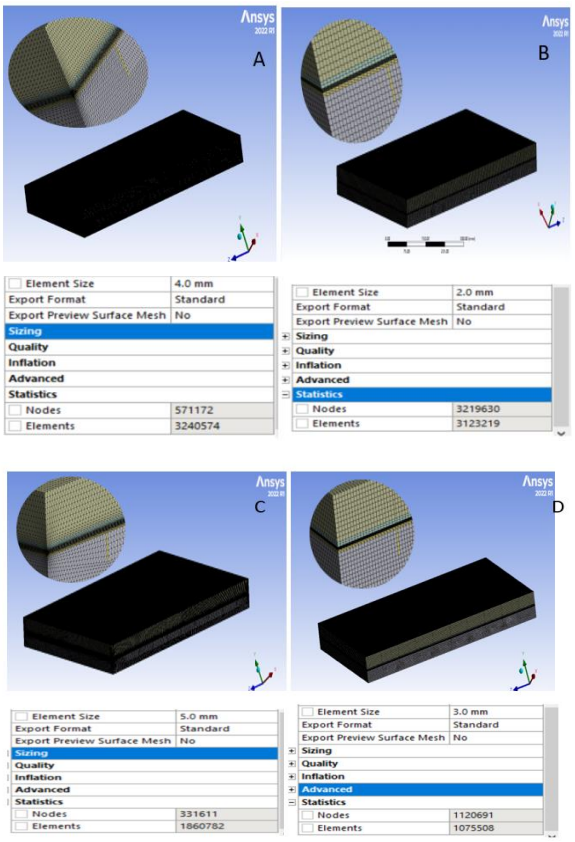

Figure A-1. Mesh size.